PERGAMON

International Journal of Solids and Structures 37 (2000) 2167–2183

INTERNATIONAL JOURNAL OF SOLIDS and STRUCTURES

www.elsevier.com/locate/ijsolstr

Perturbation boundary–finite element combined method for solving the linear creep problem

Haitian Yang, Xinglin Guo

Department of Engineering Mechanics, Dalian University of Technology, Dalian 116024, People's Republic of China

Received 20 September 1997; in revised form 14 October 1998

Abstract

This paper presents a perturbation and finite–boundary element combined approach for solving the problem of linear creep. Compared with the conventional incremental method, the field variables, without assumptions of remaining constant or varying linearly with time within a discretised time interval, can be described more precisely. The recursive formulae of perturbation for boundary–finite elements are constructed with the consideration of reinforcement. Numerical verification of the approach proposed gives good correlation against analytic solutions. This encourages the extension of the work.

Keywords: Perturbation; Finite/boundary element; Creep; Reinforcement

Nomenclature

A_r	cross-section area of reinforcement
a_0, a_1, a_2	constant coefficients
b_0 ,b_1 ,b_2	constant coefficients
$\boldsymbol{B}_i$	vector of body force
$\boldsymbol{B}_i^m$	coefficient vector of $\boldsymbol{B}_i$
$\{\boldsymbol{B}\}$	vector of body force
$\{\boldsymbol{B}\}^m$	coefficient vector of $\{\boldsymbol{B}\}$
c_1, c_2, c_3	constant coefficients
$c_{m,m-l}$	constant coefficient
$C(t)$	known function

E-mail address: haitian@dlut.edu.cn (H. Yang)

0020-7683/00/$ - see front matter
PII: S0020-7683(98)00314-X

$[D]$	constant matrix
$[\bar{D}]$	constant matrix
$D_{m,m-1}$	constant coefficient
E	Young's modulus
E_{r}	elastic modulus of reinforcement
G	shear modulus
$[G]$	coefficient matrix
$[H]$	coefficient matrix
$[\bar{H}]$	matrix of differential operators
$[K]$	stiffness matrix
L_{12}, L_{23}	segment length of reinforcement
m	expanding order of perturbation
n_i	direction cosine
$[N]$	matrix of shape function
$\boldsymbol{p}_i$	vector of traction
$\boldsymbol{p}_i^m$	coefficient vector of $\boldsymbol{p}_i$
$\bar{\boldsymbol{p}}_i$	prescribed $\boldsymbol{p}_i$ on the boundary
$\bar{\boldsymbol{p}}_i^m$	coefficient vector of $\bar{\boldsymbol{p}}_i$
p_i^*	weighted function
p_{jk}^*	weighted function
$\{\boldsymbol{p}\}$	vector of traction on the boundary
$\{\boldsymbol{p}\}^m$	coefficient vector of $\{\boldsymbol{p}\}$
$\{\bar{\boldsymbol{P}}_{\mathrm{B}}\}^m$	coefficient vector of node point traction
$\{\bar{\boldsymbol{P}}_{\mathrm{F}}\}^m$	coefficient vector of node point load
r	distance between source and field point
s	perturbation variable
t	time
t_0	starting point of time
T	size of time interval
$\boldsymbol{u}_i$	vector of displacement
$\boldsymbol{u}_i^m$	the coefficient vector of $\boldsymbol{u}_i$
$\{\boldsymbol{u}\}$	vector of displacement
$\{\boldsymbol{u}\}^m$	coefficient vector of $\{\boldsymbol{u}\}$
$\bar{\boldsymbol{u}}_i$	prescribed $\boldsymbol{u}_i$ on the boundary
$\bar{\boldsymbol{u}}_i^m$	coefficient vector of $\bar{\boldsymbol{u}}_i$
$\boldsymbol{u}_i^*$	weighted function
$\boldsymbol{u}_{ik}^*$	weighted function
$\{\bar{\boldsymbol{U}}\}$	vector of node point displacement
$\{\bar{\boldsymbol{U}}\}^m$	coefficient vector of $\{\bar{\boldsymbol{U}}\}$
$\{\bar{\boldsymbol{U}}_{\mathrm{B}}\}^m$	coefficient vector of node point displacement
$\{\bar{\boldsymbol{U}}_{\mathrm{F}}\}$	vector of node point displacement
$\{\bar{\boldsymbol{U}}_{\mathrm{F}}\}^m$	coefficient vector of node point displacement
u_1, u_2, u_3, v_1, v_2, v_3	displacement at end points of reinforcement
u_L^1, u_L^2	displacements at end points of reinforcement
x_i	coordinate index
$M\{\boldsymbol{\varepsilon}\}\}$	vector of strain
$\boldsymbol{\varepsilon}_{ij}$	strain tensor
$\boldsymbol{\varepsilon}_{ij}^m$	coefficient tensor of strain

$\boldsymbol{\varepsilon}_{\mathrm{r}}$	strain of reinforcement
$\boldsymbol{\varepsilon}_{\mathrm{r}}^{m}$	coefficient of $\boldsymbol{\varepsilon}_{\mathrm{r}}$
$\{\boldsymbol{\sigma}\}$	vector of stress
$\boldsymbol{\sigma}_{ij}$	stress tensor
$\boldsymbol{\sigma}_{ij}^{m}$	coefficient tensor of stress
$\boldsymbol{\sigma}_{\mathrm{r}}$	stress of reinforcement
$\boldsymbol{\sigma}_{\mathrm{r}}^{m}$	coefficient of $\boldsymbol{\sigma}_{\mathrm{r}}$
Γ	boundary of a domain
μ	Poisson's ratio
γ	material constant
τ_0	initial age of material
θ_{12}, θ_{23}	angles between reinforcement and X-axis
$\delta(t, \tau)$	kernel function of creep
$\varphi(t, \tau)$	known function

1. Introduction

Creep analysis plays an important role in practical engineering. One of the relevant issues, for instance, is the safe operation of concrete structures and structures built in the rock with the consideration of long-term creep deformation (see e.g. Ponter et al., 1981; Wang, 1984).

Due to the complexity of creep constitutive relations, inhomogeneity of media, as well as complex geometric shapes of structures, the solutions of creep problems are difficult to obtain analytically for most cases and computer based numerical techniques are inevitably required.

A perturbation and finite–boundary element combined technique is, therefore, developed in this paper for solving the linear creep problems. The advantages of this combination are the convenience of simultaneous discrete computing in the space and time domains and the capability of dealing with not only a single creep body but also two or more coupled creep bodies, which have different ages and arbitrary geometric shapes. Also, since the assumption (see e.g. Ouyang, 1989; Zeinkiewicz, 1975; Zhu, 1983) in conventional incremental computation that variables remain constant or change linearly in a divided time interval is not adopted, the variation of variables in the time domain can be described more precisely. Previous examples of using finite element–perturbation algorithms for the solution of non-linear problems have been presented in the literature (see e.g. Xie, 1983, 1984; Yang, 1996; Yokoo et al., 1976).

A number of numerical tests, considering time dependent boundary conditions, coupled effect of temperature and creep, reinforced structures and coupled creep bodies with different ages, etc., were implemented to verify the correctness of the model proposed in terms of comparison with analytical solutions.

2. Constitutive equation and perturbation formulae in the problem of linear creep

A number of engineering materials, such as concrete, rock, etc., can be described by the linear creep theory (see e.g. Arutyunyan, 1961; Christensen, 1982), in which, the constitutive relation can be expressed in an integral form

$$\{\boldsymbol{\varepsilon}\} = [D]\left\{\{\boldsymbol{\sigma}\}/E - \int_{\tau_0}^{t} \{\boldsymbol{\sigma}(\tau)\}\frac{\partial}{\partial\tau}\delta(t,\tau)\,\mathrm{d}\tau\right\} \tag{1}$$

where $\delta(t,\tau) = 1/E(\tau) + \varphi(\tau)(1 - \mathrm{e}^{-\gamma(t-\tau)}) - C(\tau)$, denoting the kernel function of creep, τ_0 refers to the age of materials.

Eqn (1) can be converted into a differential form, facilitating the implementation of perturbation.

Taking time derivative of first- and second-orders of eqn (1) can yield

$$\{\boldsymbol{\varepsilon}\}' = [D]\left\{\{\boldsymbol{\sigma}\}'/E(\tau) + \{\boldsymbol{\sigma}\}\left[\gamma\varphi(t) + C'(t)\right] - \int_{\tau_0}^{t} \{\boldsymbol{\sigma}(\tau)\}\gamma\mathrm{e}^{-\gamma(t-\tau)}\left[\varphi'(\tau) + \gamma\varphi'(\tau)\right]\mathrm{d}\tau\right\} \tag{2}$$

$$\{\boldsymbol{\varepsilon}\}'' + \gamma\{\boldsymbol{\varepsilon}\}' = [D]\left\{\{\boldsymbol{\sigma}\}''/E(t) + \left[\gamma\varphi(t) + C'(t) + \gamma/E(t) - E'(t)/E^2(t)\right]\{\boldsymbol{\sigma}\}' + \left[C''(t) + \gamma C'(t)\right]\{\boldsymbol{\sigma}\}\right\} \tag{3}$$

where $\{\boldsymbol{\varepsilon}\}$ and $\{\boldsymbol{\sigma}\}$ denote the vectors of strain and stress, respectively; $E(\tau)$ is the Young's modulus, $\varphi(\tau)$ and $C(\tau)$ are the known functions; γ represents a material constant; $[D]$ is a constant matrix. For the problem of plane stress, $[D]$ can be written as

$$[D] = \begin{bmatrix} 1 & -\mu & 0 \\ -\mu & 1 & 0 \\ 0 & 0 & 2(1+\mu) \end{bmatrix}$$

For the problem of plane strain, $[D]$ becomes

$$[D] = \begin{bmatrix} (1-\mu^2) & -\mu(1-\mu) & 0 \\ -\mu(1-\mu) & (1-\mu^2) & 0 \\ 0 & 0 & 2(1+\mu) \end{bmatrix}$$

where μ is the Poisson ratio.

Eqn (3), converted from eqn (1), represents the constitutive relation of creep in a differential form.

In order to describe the variation of variables in the time domain more precisely, a perturbation procedure is introduced, in which variables are expanded in the term of s defined as

$$s = (t - t_0)/T$$

where t_0 is an arbitrary starting point of time, T represents the size of a time interval. The relation of differentials between s and t can be expressed as

$$\frac{\mathrm{d}}{\mathrm{d}t} = \frac{1}{T}\frac{\mathrm{d}}{\mathrm{d}s}$$

$$\frac{\mathrm{d}^2}{\mathrm{d}t^2} = \frac{1}{T^2}\frac{\mathrm{d}^2}{\mathrm{d}s^2}$$

Expanding the vectors of stress and strain in a discretised time interval can yield

$$\{\boldsymbol{\varepsilon}\} = \Sigma\{\boldsymbol{\varepsilon}\}^m s^m \tag{4}$$

$$\{\boldsymbol{\sigma}\} = \Sigma\{\boldsymbol{\sigma}\}^m s^m \tag{5}$$

where $\{\boldsymbol{\varepsilon}\}^m$ and $\{\boldsymbol{\sigma}\}^m$ denote the coefficient vectors of strain and stress, respectively, superscript m refers to the order of perturbation.

In a discretised time interval, we can assume

$$E = a_0 + a_1 s + a_2 s^2 \tag{6}$$

$$\varphi = b_0 + b_1 s + b_2 s^2 \tag{7}$$

$$C = c_1 + c_2 s + c_3 s^2 \tag{8}$$

where a_0, a_1, a_2, b_0, b_1, b_2, c_1, c_2 and c_3 are the constant coefficients associated with material properties.

Substituting eqns (4)–(8) for eqns (1) and (2) and letting $t = \tau_0$ can yield

$$\{\boldsymbol{\varepsilon}\}^0 = [D]/a_0\{\boldsymbol{\sigma}\}^0 \tag{9}$$

$$\{\boldsymbol{\varepsilon}\}^1 = [D]\left\{\{\boldsymbol{\sigma}\}^1/a_0 + T(\gamma b_0 + c_1/T)\{\boldsymbol{\sigma}\}^0\right\} \tag{10}$$

A perturbation based recursive constitutive relation can be obtained by a substitution of eqns (4)–(8) for eqn (3), having the form

$$\{\boldsymbol{\sigma}\} = [\bar{D}]\left\{\{\boldsymbol{\varepsilon}\}^m + \sum_{k=1}^{m} c_{m,m-k}\{\boldsymbol{\varepsilon}\}^{m-k}\right\} \tag{11}$$

where $c_{m,m-k}$ can be determined by material parameters

$$[\bar{D}] = a_0[D]^{-1}$$

A recursive relation between coefficient vectors of strain and stress is specified by eqn (11).

3. Perturbation formulae of boundary element method

In the derivation of perturbation–boundary element based formulae, an expansion similar to Section 2 needs to be implemented to governing equations specified by

$$\boldsymbol{\sigma}_{ij,j} + \boldsymbol{B}_i = 0 \quad \text{(equilibrium relation)} \tag{12}$$

$$\boldsymbol{\varepsilon}_{ij} = (\boldsymbol{u}_{i,j} + \boldsymbol{u}_{j,i})/2 \quad \text{(strain–displacement relation)} \tag{13}$$

$$\boldsymbol{u}_i = \bar{\boldsymbol{u}}_i \quad \text{(displacement boundary condition)} \quad \text{on } \Gamma_u \tag{14}$$

$$\boldsymbol{p}_i = \bar{\boldsymbol{p}}_i \quad \text{(stress boundary condition)} \quad \text{on } \Gamma_\sigma \tag{15}$$

where $\boldsymbol{\sigma}_{ij}$ and $\boldsymbol{\varepsilon}_{ij}$ denote the stress and strain tensors, respectively; $\boldsymbol{u}_i$ is the vector of displacement; $\boldsymbol{p}_i$ represents the vector of traction; $\bar{\boldsymbol{u}}_i$, $\bar{\boldsymbol{p}}_i$ are the prescribed values of $\boldsymbol{u}_i$ and $\boldsymbol{p}_i$ on the boundaries.

$\Gamma = \Gamma_u + \Gamma_\sigma$ represents the boundary of a domain, subscript u and σ refer to the displacement and stress, respectively.

The variables in eqns (12)–(15) can be expanded in the term of s, having the form

$$\boldsymbol{\varepsilon}_{ij} = \boldsymbol{\Sigma}\boldsymbol{\varepsilon}_{ij}^m s^m \tag{16}$$

$$\boldsymbol{\sigma}_{ij} = \boldsymbol{\Sigma}\boldsymbol{\sigma}_{ij}^m s^m \tag{17}$$

$$\boldsymbol{B}_i = \boldsymbol{\Sigma}\mathbf{B}_i^m s^m \tag{18}$$

$$\boldsymbol{u}_i = \boldsymbol{\Sigma}\mathbf{u}_i^m s^m \tag{19}$$

$$\boldsymbol{p}_i = \boldsymbol{\Sigma}\mathbf{p}_i^m s^m \tag{20}$$

$$\bar{\boldsymbol{u}}_i = \boldsymbol{\Sigma}\bar{\mathbf{u}}_i^m s^m \tag{21}$$

$$\bar{\boldsymbol{p}}_i = \boldsymbol{\Sigma}\bar{\mathbf{p}}_i^m s^m \tag{22}$$

where $\boldsymbol{\varepsilon}_{ij}^m$ and $\boldsymbol{\sigma}_{ij}^m$ represent the coefficient tensors of strain and stress; $\boldsymbol{p}_i^m$, $\bar{\boldsymbol{p}}_i^m$, $\boldsymbol{u}_i^m$ and $\bar{\boldsymbol{u}}_i^m$ are the coefficient vectors of traction and displacement, respectively.

Substituting eqns (16)–(22) for eqns (12)–(15) can yield a group of perturbation based governing equations, having the form

$$\boldsymbol{\sigma}_{ij,j}^m + \boldsymbol{B}_i^m = 0 \tag{23}$$

$$\boldsymbol{\varepsilon}_{ij}^m = \left(\boldsymbol{u}_{i,j}^m + \boldsymbol{u}_{j,i}^m\right)/2 \tag{24}$$

$$\boldsymbol{u}_i^m = \bar{\boldsymbol{u}}^m \quad \text{on } \Gamma_u \tag{25}$$

$$\boldsymbol{p}_i^m = \bar{\boldsymbol{p}}_i^m \quad \text{on } \Gamma_\sigma \tag{26}$$

Employing the weighting technique to eqns (23), (25) and (26) then yields

$$\int_\upsilon \left(\boldsymbol{\sigma}_{ij,j}^m + \boldsymbol{B}_i^m\right)u_i^* \,\mathrm{d}\upsilon + \int_{\Gamma_u} \left(\boldsymbol{u}_i^m - \bar{\boldsymbol{u}}_i^m\right)p_i^* \,\mathrm{d}\Gamma - \int_{\Gamma_\sigma} \left(\boldsymbol{p}_i^m - \bar{\boldsymbol{p}}_i^m\right)u_i^* \,\mathrm{d}\Gamma = 0 \tag{27}$$

where u_i^* and p_i^* denote weighting functions.

By utilizing the theorem of integration by part and the relation of eqn (11) in the tensor form, the first term in eqn (27), if $\boldsymbol{B}_i = 0$, can be written as

$$\int_\upsilon \boldsymbol{\sigma}_{ij,j}^m u_i^* \,\mathrm{d}\upsilon = \int_\Gamma \boldsymbol{p}_i^m u_i^* \,\mathrm{d}\Gamma - \int_\Gamma \left(\boldsymbol{u}_i^m + \Sigma c_{m,m-l}\boldsymbol{u}_i^{m-l}\right)p_i^* \,\mathrm{d}\Gamma + \int_\upsilon \left(\boldsymbol{u}_i^m + \Sigma c_{m,m-l}\boldsymbol{u}_i^{m-l}\right)\boldsymbol{\sigma}_{ij,j} \,\mathrm{d}\upsilon \tag{28}$$

Substituting eqn (28) for eqn (27) then yields

$$\int_{\Gamma} \boldsymbol{p}_i^m u_i^m \, \mathrm{d}\upsilon - \int_{\Gamma} \boldsymbol{u}_i^m p_i^* \, \mathrm{d}\Gamma + \int_{\upsilon} \boldsymbol{u}_i^m \boldsymbol{\sigma}_{ij,j}^* \, \mathrm{d}\upsilon = \int_{\Gamma} p_i^* \Sigma c_{m,m-l} \boldsymbol{u}_i^{m-l} \, \mathrm{d}\Gamma - \int_{\upsilon} \boldsymbol{\sigma}_{ij,j}^* \Sigma c_{m,m-l} \boldsymbol{u}_i^{m-l} \, \mathrm{d}\upsilon \tag{29}$$

For the 2-D problems, the weighting functions can be specified by

$$u_{lk}^* = \frac{1}{8\pi G(1-\mu)} \left\{ (3-4\mu) \ln \frac{1}{r} \delta_{lk} + \frac{\partial r}{\partial x_l} \frac{\partial r}{\partial x_k} \right\} \tag{30}$$

$$p_{lk}^* = \frac{1}{4\pi(1-\mu)r} \left\{ \frac{\partial r}{\partial n} \left[(1-2\mu)\delta_{lk} + 2\frac{\partial r}{\partial x_l} \frac{\partial r}{\partial x_k} \right] - (1-2\mu) \left[\frac{\partial r}{\partial x_l} n_k - \frac{\partial r}{\partial x_k} n_l \right] \right\} \tag{31}$$

where G represents the shear modulus, r denotes the distance between source point and field points, n_i refers to the direction cosines of the outward normal to the boundary. u_{lk}^* and p_{lk}^* represent the weighting functions of displacement and traction, respectively.

Substituting eqns (30) and (31) for eqn (29) and discretising integration on the boundary (see e.g. Brebbia, 1980) then yields

$$[G]\{\bar{\boldsymbol{P}}_{\mathrm{B}}\}^m = [H]\left(\{\bar{\boldsymbol{U}}_{\mathrm{B}}\}^m + \Sigma c_{m,m-l} \{\bar{\boldsymbol{U}}_{\mathrm{B}}\}^{m-l} \right) \tag{32}$$

where $\{\bar{\boldsymbol{P}}_{\mathrm{B}}\}^m$ and $\{\bar{\boldsymbol{U}}_{\mathrm{B}}\}^m$ represent the coefficient vectors of nodal point traction and displacement on the boundary, $[G]$ and $[H]$ are the coefficient matrices, subscript 'B' refers to the boundary element.

Eqn (32) represents a perturbation–boundary element based recursive formula.

3.1. Numerical example

The time-dependent displacement of a ring subjected to an internal uniform pressure in the infinite viscoelastic medium, as shown in Fig. 1, is investigated. The computing parameters are as follows: $a = 300$ cm; $\gamma = 3.0093 \times 10^{-7}$/s; $\varphi = 0.0005$ cm^2/kg; and $E = 2 \times 10^5$ kg/cm^2. In this example, both time-

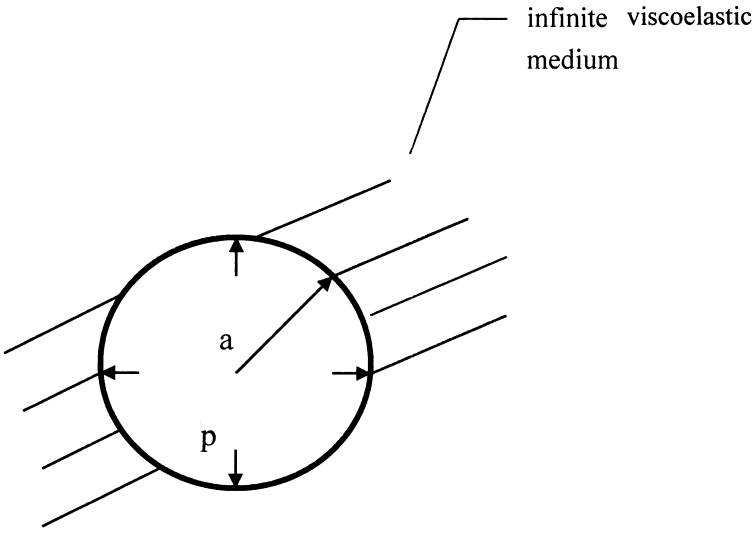

Fig. 1. A ring in the infinite viscoelastic medium.

Table 1
Solution of displacement ($r = a$, $p = 1000$ kg/cm^2, $m = 3$, $T_m = 5$ days)

t (day)	u^* (cm)	u^{**} (cm)
1	0.05081	0.049813
5	0.18199	0.17841
10	0.33156	0.32502
15	0.4622	0.45702
20	0.58746	0.57587
25	0.69661	0.68286
30	0.79489	0.77919
35	0.88336	0.86593
40	0.96302	0.94401
50	1.10993	1.07761
60	1.20978	1.1859

dependent and independent boundary conditions are taken into account via internal pressure p shown in Fig. 1. Numerical comparison are exhibited in Tables 1 and 2 where subscript 'm' refers to the minimum size of the time step, '*' denotes analytical solutions and '**' is given by the present paper.

4. Perturbation formulae of finite element

Similar to Section 3, a perturbation procedure is also required to be implemented to governing equations. Expansion starts from eqn (12) in a weak form on the basis of the virtual displacement principle, having the form

$$\int_{\upsilon} \delta\{\varepsilon\}^{\mathrm{T}}\{\boldsymbol{\sigma}\}\,\mathrm{d}\upsilon = \int_{\upsilon} \delta\{\boldsymbol{u}\}^{\mathrm{T}}\{\boldsymbol{B}\}\,\mathrm{d}\upsilon + \int_{\Gamma_\sigma} \delta\{\boldsymbol{u}\}^{\mathrm{T}}\{\boldsymbol{p}\}\,\mathrm{d}\Gamma \tag{33}$$

where $\delta\{\boldsymbol{\varepsilon}\}$ and $\delta\{\boldsymbol{u}\}$ represent the vectors of virtual strain and displacement; $\{\boldsymbol{B}\}$ and $\{\boldsymbol{p}\}$ represent the vectors of body force and traction, respectively and can be expanded in the term of s, having the form

Table 2
Solution of displacement ($r = a$, $p = (1000 - t)$ kg/cm^2, $m = 3$, $T_m = 5$ days)

t (day)	u^* (cm)	u^{**} (cm)
1	0.050474	0.049478
5	0.18149	0.17791
10	0.32977	0.32326
15	0.46243	0.4566
20	0.58102	0.56956
25	0.68696	0.67341
30	0.78149	0.76608
35	0.86578	0.84869
40	0.94081	0.92225
50	1.06677	1.04571
60	1.16567	1.14267

$$\{\boldsymbol{B}\} = \Sigma\{\boldsymbol{B}\}^m s^m \tag{34}$$

$$\{\boldsymbol{p}\} = \Sigma\{\boldsymbol{p}\}^m s^m \tag{35}$$

The vector of displacement $\{\boldsymbol{u}\}$ can also be expanded as

$$\{\boldsymbol{u}\} = \Sigma\{\boldsymbol{u}\}^m s^m \tag{36}$$

where $\{\boldsymbol{B}\}^m$, $\{\boldsymbol{p}\}^m$ and $\{\boldsymbol{u}\}^m$ represent coefficient vectors of $\{\boldsymbol{B}\}$, $\{\boldsymbol{p}\}$ and $\{\boldsymbol{u}\}$, respectively.

Substituting eqns (5), (34) and (35) for eqn (33) can yield

$$\int_\upsilon \delta\{\boldsymbol{\varepsilon}\}^{\mathrm{T}}\{\boldsymbol{\sigma}\}^m \,\mathrm{d}\upsilon = \int_\upsilon \delta\{\boldsymbol{u}\}^{\mathrm{T}}\{\boldsymbol{B}\}^m \,\mathrm{d}\upsilon + \int_\Gamma \delta\{\boldsymbol{u}\}^{\mathrm{T}}\{\boldsymbol{p}\}^m \,\mathrm{d}\Gamma \tag{37}$$

By utilizing eqns (11) and (13) in the form of a vector, i.e. $\{\boldsymbol{\varepsilon}\} = [\bar{H}]\{\boldsymbol{u}\}$, eqn (37) can be further described as

$$\begin{aligned}\int_\upsilon \delta\{\boldsymbol{\varepsilon}\}^{\mathrm{T}}\{\boldsymbol{\sigma}\}^m \,\mathrm{d}\upsilon &= \int \delta\{\boldsymbol{\varepsilon}\}^{\mathrm{T}}[\bar{D}]\left(\{\boldsymbol{\varepsilon}\}^m + \Sigma c_{m,m-k}\{\boldsymbol{\varepsilon}\}^{m-k}\right)\mathrm{d}\upsilon \\ &= \int \delta\{\boldsymbol{\varepsilon}\}^{\mathrm{T}}[\bar{D}][\bar{H}]\left(\{\boldsymbol{u}\}^m + \Sigma c_{m,m-k}\{\boldsymbol{u}\}^{m-k}\right)\mathrm{d}\upsilon \\ &= \int_\upsilon \delta\{\boldsymbol{u}\}^{\mathrm{T}}\{\boldsymbol{B}\}^m \,\mathrm{d}\upsilon + \int_\Gamma \delta\{\boldsymbol{u}\}^{\mathrm{T}}\{\boldsymbol{p}\}^m \,\mathrm{d}\Gamma\end{aligned} \tag{38}$$

where $[\bar{H}]$ is a matrix of differential operators, which, for 2-D problems, can be defined as

$$[\bar{H}] = \begin{bmatrix} \partial/\partial x & 0 \\ 0 & \partial/\partial y \\ \partial/\partial y & \partial/\partial x \end{bmatrix} \tag{39}$$

Domain υ can be discretised into a number of elements where $\{\boldsymbol{u}\}^m$ is represented by

$$\{\boldsymbol{u}\}^m = [N]\left\{\bar{\boldsymbol{U}}\right\}^m \tag{40}$$

where $[N]$ refers to a matrix of shape functions, $\{\bar{\boldsymbol{U}}\}^m$ denotes the value of $\{\boldsymbol{u}\}^m$ at node points of an element.

Substituting eqn (40) for eqn (38) and assembling over all the elements can yield (see e.g. Zeinkiewicz, 1971)

$$[K]\left\{\bar{\boldsymbol{U}}_{\mathrm{F}}\right\}^m = \left\{\bar{\boldsymbol{P}}_{\mathrm{F}}\right\}^m - [K]\Sigma c_{m,m-k}\left\{\bar{\boldsymbol{U}}_{\mathrm{F}}\right\}^{m-k} \tag{41}$$

where $\{\bar{\boldsymbol{U}}_{\mathrm{F}}\}^m$ refers to a global coefficient vector of displacement on node points, $[K]$ denotes a 'stiffness' matrix and $\{\bar{\boldsymbol{P}}_{\mathrm{F}}\}^m$ is a global coefficient vector of equivalent node point loads, converted by

$$\{\bar{\boldsymbol{P}}\}^m = \Sigma\int_\upsilon [N]^{\mathrm{T}}\{\boldsymbol{B}\}^m \,\mathrm{d}\upsilon + \Sigma\int_{\Gamma_\sigma} [N]^{\mathrm{T}}\{\boldsymbol{p}\}^m \,\mathrm{d}\Gamma \tag{42}$$

subscript 'F' refers to 'Finite element'.

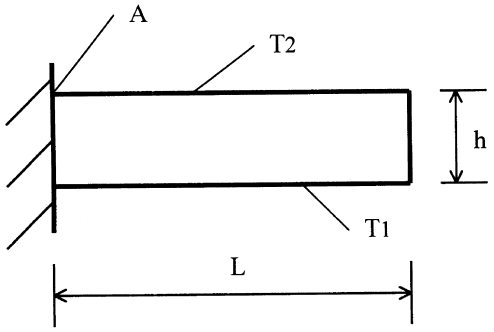

Fig. 2. A concrete beam.

4.1. Numerical example

This example, with respect to the creep of a concrete beam shown in Fig. 2, is given to describe a decrease of stress caused by a un-uniform temperature field, varying linearly along the height of the beam. The coupled effect of temperature and creep on the stress is analysed by considering temperature strain as an initial one. The computing parameters are listed as follows:

$$T_1 = 15^\circ\mathrm{C},\ T_2 = -5^\circ\mathrm{C};$$
$$E = 200{,}000\ \mathrm{kg/cm^2};$$
$$\tau_0 = 14\ \text{days};$$
$$\gamma = 3.0093 \times 10^{-7}/\mathrm{s};$$
$$\varphi(\tau) = (A_1/\tau + C_0);$$
$$C_0 = 0.5 \times 10^{-5}\ \mathrm{cm^2/kg},\ A_1 = 4.1645\ \mathrm{cm^2/kg\ s},\ L = 200\ \mathrm{cm},\ h = 20.0\ \mathrm{cm}.$$

The numerical comparison is exhibited in Table 3 in terms of stress at point A shown in Fig. 2.

5. The stiffness matrix of reinforcement

Reinforcement is widely used in many aspects of practical engineering and has to be considered in the creep analysis since it often plays an important role affecting the creep behavior of matrix materials. In this section, a parent element based stiffness matrix of reinforcement is constructed for the use of perturbation based computation.

An eight-node isoparametric element is considered as a parent element where a length of reinforcement locates on it. The following assumptions are adopted in the derivation.

Table 3
The stress variation with time (at point A, $m = 3$, $T_m = 5$)

t (day)	14	20	28	45	90	150
$(\sigma(t)/\sigma(\tau_0))^*$	1.0	0.6963	0.4731	0.2922	0.2281	0.2227
$\sigma(t)/\sigma(\tau_0))^{**}$			0.479	0.297	0.233	0.233

Where '**' refers to the solutions obtained by Arutyunyan (1961), '$*$' represents those given by the present paper.

1. There is no relative sliding between the parent element and the reinforcement.
2. The strain of reinforcement is within the elastic limit.
3. Only axial stress of reinforcement is considered.
4. The reinforcement is located on a side of the parent element. In the derivation it is assumed to be on the side 1–2–3.

The reinforcement, is divided into two parts, from node points 1–2 and 2–3, respectively, as shown in Fig. 3. They are, firstly considered as linear elements, respectively, then fixed together.

The displacement of nodes 1 and 2 along the reinforcement can be described as

$$u_{L1} = u_1 \cos\theta_{12} + v_1 \sin\theta_{12} \tag{43}$$

$$u_{L2} = u_2 \cos\theta_{12} + v_2 \sin\theta_{12} \tag{44}$$

The strain in segment 1–2 can be written as

$$\varepsilon_{r12} = \{ -\cos\theta_{12}, -\sin\theta_{12}, \cos\theta_{12}, \sin\theta_{12} \} \begin{bmatrix} u_1 \\ v_1 \\ u_2 \\ v_2 \end{bmatrix} / L_{12} \tag{45}$$

where L_{12} is the length of segment 1–2.

A similar formula can also be obtained on segment 2–3, having the form

$$\varepsilon_{r23} = \{ -\cos\theta_{23}, -\sin\theta_{23}, \cos\theta_{23}, \sin\theta_{23} \} \begin{bmatrix} u_2 \\ v_2 \\ u_3 \\ v_3 \end{bmatrix} / L_{23} \tag{46}$$

where u_1, u_2, u_3, v_1, v_2 and v_3 represent the displacements of node points 1–3 under the global coordinate system, u_L^1 and u_L^2 denote the displacements of node points 1 and 2 under the local coordinate system, L_{23} is the length of segment 2–3, and subscript 'r' refers to reinforcement.

Based on the forenamed assumption, the constitutive relation of reinforcement can be written as

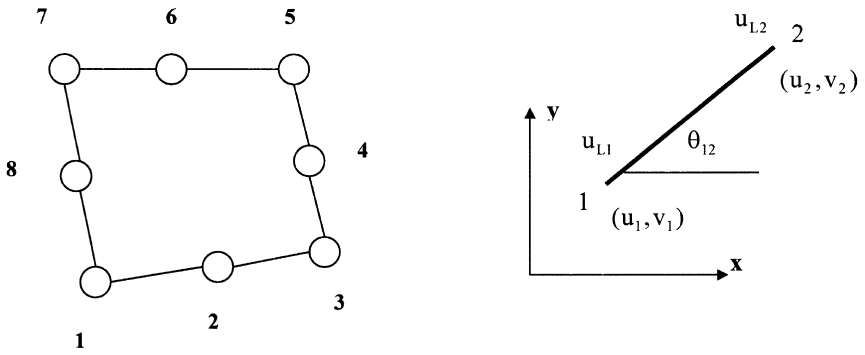

Fig. 3. An element with reinforcement.

$$\boldsymbol{\sigma}_{\mathrm{r}} = E_{\mathrm{r}}\boldsymbol{\varepsilon}_{\mathrm{r}} \tag{47}$$

where E_{r} is the elastic modulus of reinforcement, $\boldsymbol{\sigma}_{\mathrm{r}}$ and $\boldsymbol{\varepsilon}_{\mathrm{r}}$ representing the stress and strain of a reinforcement, respectively, can be expanded in the terms of s, having the form

$$\boldsymbol{\sigma}_{\mathrm{r}} = \Sigma\boldsymbol{\sigma}_{\mathrm{r}}^{m} s^{m} \tag{48}$$

$$\boldsymbol{\varepsilon}_{\mathrm{r}} = \Sigma\varepsilon_{\mathrm{r}}^{m} s^{m} \tag{49}$$

Substituting eqns (48) and (49) for eqn (47) then yields

$$\boldsymbol{\sigma}_{\mathrm{r}}^{m} = E_{\mathrm{r}}\boldsymbol{\varepsilon}_{\mathrm{r}}^{m} \tag{50}$$

The contribution of a reinforcement can be considered by adding a term $\int A_{\mathrm{r}}\delta\boldsymbol{\varepsilon}_{\mathrm{r}}\boldsymbol{\sigma}_{\mathrm{r}}\,\mathrm{d}L$ into eqn (33), which will lead to an additional term $\int A_{\mathrm{r}}\delta\boldsymbol{\varepsilon}_{\mathrm{r}}\boldsymbol{\sigma}_{\mathrm{r}}^{m}\,\mathrm{d}L$ in eqn (37) where $\delta\boldsymbol{\varepsilon}_{\mathrm{r}}$ represents the virtual strain of reinforcement and A_{r} refers to the cross-section area of reinforcement.

By substituting $\boldsymbol{\sigma}_{\mathrm{r}}^{m}$ with the coefficient vector of displacement at node points in virtue of eqns (45), (46) and (50), the contribution of reinforcements can appear in eqn (41) in the term of $\{\bar{\boldsymbol{U}}_{\mathrm{F}}\}$ and a reinforcement related additional stiffness matrix will be generated and assembled into $[K]$. At the element level, stiffness matrices of segments 1–2 and 2–3 can be expressed as

$$\begin{bmatrix} -\cos\theta_{12} \\ -\sin\theta_{12} \\ \cos\theta_{12} \\ \sin\theta_{12} \end{bmatrix} \left\{ -\cos\theta_{12},\ -\sin\theta_{12}, \cos\theta_{12}, \sin\theta_{12} \right\} E_{\mathrm{r}}A_{\mathrm{r}}/L_{12} \tag{51}$$

$$\begin{bmatrix} -\cos\theta_{23} \\ -\sin\theta_{23} \\ \cos\theta_{23} \\ \sin\theta_{23} \end{bmatrix} \left\{ -\cos\theta_{23},\ -\sin\theta_{23}, \cos\theta_{23}, \sin\theta_{23} \right\} E_{\mathrm{r}}A_{\mathrm{r}}/L_{12} \tag{52}$$

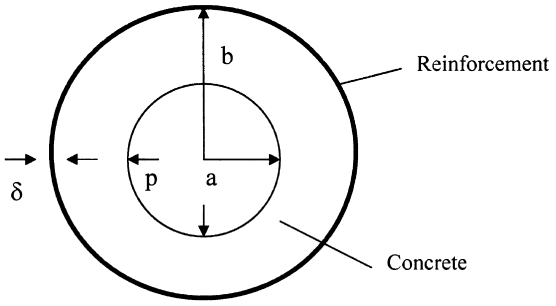

Fig. 4. A concrete cylinder with reinforcement.

Table 4
The stress variation in reinforcement with time ($m = 3$, $T_m = 5$ days)

t (day)	$(\sigma(t)/\sigma(\tau_0))$ (Arutyunyan, 1961)	$(\sigma(t)/\sigma(\tau_0))$
170	2.707	2.73

5.1. Numerical example

This example is employed to verify the correctness of the reinforcement element derived above, in which a numerical solution for a reinforced concrete cylinder subjected to an internal uniform pressure, as shown in Fig. 4, is given in Table 4. Computing parameters are as follows:

$$a = 200 \text{ cm}, b = 260 \text{ cm}, E_c = 2 \times 10^5 \text{ kg/cm}^2, E_r = 2 \times 10^6 \text{ kg/cm}^2, \tau_0 = 28 \text{ days};$$

$$\gamma = 3.0093 \times 10^{-7}/\text{s}, \varphi(\tau) = (A_1/\tau + C_0), C_0 = 0.9 \times 10^{-5} \text{ cm}^2/\text{kg}, A_1 = 4.1645 \text{ cm},^2/\text{kg s}.$$

Subscript 'c' refers to concrete.

6. Boundary and finite element coupled perturbation formulae

The idea of combining both BEM and FEM with perturbation techniques is of considerable interest in some practical problems. In the numerical analysis of an underground tunnel, for example, FEM can be employed in the near-field, facilitating dealing with reinforcement and reinforced concrete lining, etc., farfield analysis can be carried out by BEF to reduce the number of unknowns. In this section, BEM–FEM coupled, recursive perturbation formulae are derived.

Assume that there are two regions, one that can include reinforcements in it, is to be investigated by FEM and another one by BEM. The variables on the interface of these two regions are described with superscript 'I'. Superscript and subscript 'F' and 'B' are employed to denote the internal variables in FEM and BEM regions, respectively.

By utilizing the conditions of equilibrium and compatibility on the interface, reorganizing eqns (32) and (41) can yield

$$\left(-H^{\mathrm{I}}, -H_{\mathrm{B}}, G^{\mathrm{I}}\right)\begin{pmatrix}\boldsymbol{U}^{\mathrm{I}}\\ \boldsymbol{U}^{\mathrm{B}}\\ \boldsymbol{P}^{\mathrm{I}}\end{pmatrix}^{m} = -G_{\mathrm{B}}\boldsymbol{P}_{\mathrm{B}}^{m} + \left(H^{\mathrm{I}}, H_{\mathrm{B}}\right)\Sigma D_{m,m-k}\begin{pmatrix}\boldsymbol{U}^{\mathrm{I}}\\ \boldsymbol{U}^{\mathrm{B}}\end{pmatrix}^{m-k} \tag{53}$$

and

$$\left(K^{\mathrm{I}}, K_{\mathrm{F}}, M\right)\begin{pmatrix}\boldsymbol{U}^{\mathrm{I}}\\ \boldsymbol{U}^{\mathrm{F}}\\ \boldsymbol{P}^{\mathrm{I}}\end{pmatrix}^{m} = \bar{\boldsymbol{P}}_{\mathrm{F}}^{m} + \left(K^{I'}, K_{\mathrm{F}}'\right)\Sigma c_{m,m-k}\begin{pmatrix}\boldsymbol{U}^{\mathrm{I}}\\ \boldsymbol{U}_{\mathrm{F}}\end{pmatrix}^{m-k} \tag{54}$$

where G_{B}, G^{I}, H^{I}, H_{B}, K^{I}, K_{F}, $K^{\mathrm{I}'}$ and K_{F}' are known sub-matrices; $(\boldsymbol{U}^{\mathrm{I}})^m$, $(\boldsymbol{U}^{\mathrm{F}})^m$, $(\boldsymbol{U}^{\mathrm{B}})^m$, $(\boldsymbol{P}^{\mathrm{I}})^m$, $\bar{\boldsymbol{P}}_{\mathrm{F}}^m$ and

$\boldsymbol{P}_{\mathrm{B}}^{m}$ represent relevant sub-coefficient vectors. M denotes a matrix generated in transforming distributive traction on the interface into FEM required 'equivalent node point lodes'. $D_{m,m-k}$ and $C_{m,m-k}$ here refer to the materials related coefficients in BE and FE regions, respectively.

Eqns (53) and (54) represent BE–FE coupled recursive perturbation formulae and needs to be solved simultaneously. For a special case where

$$\left(\boldsymbol{P}_{\mathrm{B}}^{m},(\boldsymbol{P}^{\mathrm{I}})^{m}\right)^{\mathrm{T}}=(\boldsymbol{P}^{\mathrm{I}})^{m}$$

and

$$\left(\boldsymbol{U}_{\mathrm{B}}^{m},(\boldsymbol{U}^{\mathrm{I}})^{m}\right)^{\mathrm{T}}=(\boldsymbol{U}^{\mathrm{I}})^{m}$$

Eqn (53) becomes

$$(\boldsymbol{P}^{\mathrm{I}})^{m}=\left[\boldsymbol{G}_{\mathrm{B}}^{\mathrm{I}}\right]^{-1}\left[H_{\mathrm{B}}^{\mathrm{I}}\right]\left\{\left\{\boldsymbol{U}^{\mathrm{I}}\right\}^{m}+\Sigma D_{m,m-k}\left\{\boldsymbol{U}^{\mathrm{I}}\right\}^{m-k}\right\} \tag{55}$$

Substitution of eqn (55) for eqn (54) then yields

$$[K_{\mathrm{F}}]\left\{\boldsymbol{U}^{\mathrm{F}}\right\}^{m}+\left\{\left[K_{\mathrm{F}}^{\mathrm{I}}\right]+[M]\left[G_{\mathrm{B}}^{\mathrm{I}}\right]^{-1}\left[H_{\mathrm{B}}^{\mathrm{I}}\right]\right\}\left\{\boldsymbol{U}^{\mathrm{I}}\right\}^{m}=\bar{\boldsymbol{P}}_{\mathrm{F}}^{m}$$

$$-\left[K_{\mathrm{F}}^{\mathrm{I}'}\quad K_{\mathrm{F}}'\right]\Sigma c_{m,m-k}\begin{pmatrix}\boldsymbol{U}^{\mathrm{F}}\\ \boldsymbol{U}_{\mathrm{I}}\end{pmatrix}^{m-k}-[M]\left[G_{\mathrm{B}}^{\mathrm{I}}\right]^{-1}\Sigma D_{m,m-k}\left\{\boldsymbol{U}^{\mathrm{I}}\right\}^{m-k} \tag{56}$$

6.1. Numerical example

(1) A coupled **BE-FE** perturbation scheme is implemented in this example to investigate the variations of displacement and stress in a reinforced concrete lining shown in Fig. 5, which is subjected to a uniform radial pressure and locates in an infinite elastic medium. BEM and FEM are employed in the areas of infinite elastic medium and reinforced concrete lining, respectively. The solutions, as exhibited in Table 5, are compared with those given by Wu (1955) and the FE perturbation technique presented in Section 3. The computing parameters are defined as:

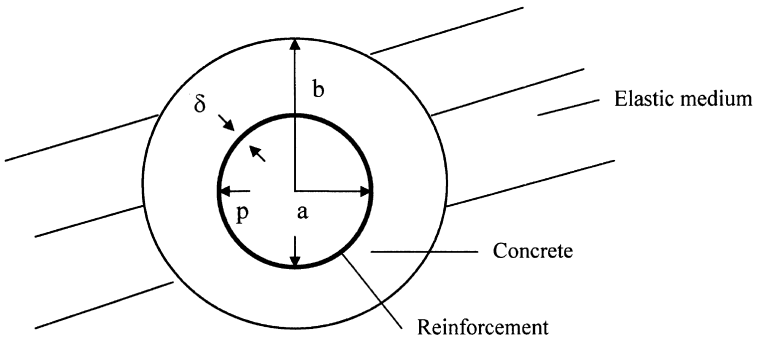

Fig. 5. A concrete cylinder with reinforcement in the infinite elastic medium.

Table 5
The variations of stress and displacement with time ($m = 3,\ T_m = 5$ days)

t (day)	$u(t)/u(\tau_0)$			$\sigma_r(t)/\sigma(\tau_0)$		
	Wu (1955)	FEM	FEM–BEM	Wu (1955)	FEM	FEM–BEM
180	1	1	1	1	1	1
210	1.2683	1.2930	1.3045	1.267	1.2932	1.3046
330	1.405	1.438	1.4747	1.42	1.4381	1.4751

$$a = 200\ \text{cm},\ b = 300\ \text{cm},\ E_c = 0.39 \times 10^5\ \text{kg/cm}^2,\ E_r = 2 \times 10^6\ \text{kg/cm}^2,\ \tau_0 = 180\ \text{days};$$

$$\gamma = 3.472 \times 10^{-7}/\text{s},\ p = 10\ \text{kg/cm}^2,\ G_e = 0.7 \times 10^5\ \text{kg/cm}^2,\ \delta = 0.6\ \text{cm},\ \mu_c = 0.3,\ \mu_e = 0.3;$$

$$\varphi(\tau) = \left(4450/\left(\tau^2 + 3030\right) + 0.28\right) \times 10\ \text{cm}^2/\text{kg};$$

where subscripts 'c' and 'e' refer to the concrete and elastic medium, respectively.

By comparison with the BE–FE coupled perturbation scheme, the other two solutions are numerically, a little smaller. The reason for this is that some assumptions were adopted by Wu (1955) and a simplified fixed boundary condition is used in FE analysis, simulating an infinite domain by a finite one.

(2) An excavation effect is simulated in this example, in which a concrete lining, as shown in Fig. 6. is assumed to be attached on the infinite viscoelastic rock five days after excavating, p in Fig. 6 refers to the excavating stress. FEM and BEM are employed in the areas of concrete lining and infinite rock, respectively. A comparison of displacement solution at $r = a$ is presented in Tables 6 and 7 where subscript 'u' refers to 'uniform size of time step'. The creep kernel functions of concrete and rock are described as:

$$\delta_c(t, \tau) = \left(0.5 \times 10^{-5} + 0.5 \times 10^{-5}\left(1 - e^{-2.8935 \times 10^{-7}(t-\tau)}\right)\right)\ \text{cm}^2/\text{kg};$$

$$\delta_R(t, \tau) = \left(10^{-4} + 10^{-4}\left(1 - e^{-2.3148 \times 10^{-7}(t-\tau)}\right)\right)\ \text{cm}^2/\text{kg}.$$

Other computing parameters are listed below

$$a = 500\ \text{cm},\ b = 470\ \text{cm},\ \tau_0 = 40\ \text{days},\ \mu_c = 0.3,\ \mu_R = 0.3,\ p = -10\ \text{kg/cm}^2.$$

Subscript 'R' refers to rock.

Two examples in this section show the capability of the presented approach to deal with coupled

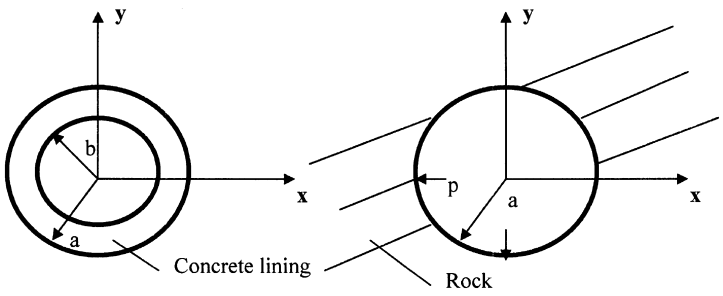

Fig. 6. A concrete lining in the infinite viscoelastic rock.

Table 6
The variation of displacement ($r = a$) with time $m = 4$, $T_u = 10$ days

t (day)	Pan (1980)	FEM	FEM–BEM
40	0	0	0
50	0.0734	0.0707	0.07392
60	0.1153	0.1092	0.1150
70	0.1406	0.1333	0.1413
80	0.1604	0.1500	0.1598

Table 7
The variation of displacement ($r = a$, $m = 3$)

t (day)	Pan (1980)	FEM–BEM ($T_u = 10$ days)	FEM–BEM ($T_u = 5$ days)
40	0	0	0
50	0.0734	0.07509	0.07392
60	0.1153	0.1222	0.1168
70	0.1406	0.1533	0.1442
80	0.1604	0.1747	0.1631

creep bodies. It is again observed in example 2 that the FE perturbation based solution is less accurate than that of the BE–FE coupled perturbation scheme due to the reason mentioned above.

7. Discussion and conclusion

The size of the time step and the number of the perturbation order are two major issues relevant to the computing in the time domain. At the initial stage where creep usually develops rapidly, either a relatively smaller size for a fixed number of the perturbation order, or a relatively higher number for specified sizes of time steps, needs to be adopted. In this paper, different sizes of time steps are employed in the whole computation of time domain with a specified number of the perturbation order. As an extension of the present work, a perturbation based self-adaptive algorithm in the time domain is being developed by the author for the solution of the coupled heat and the moisture transfer problem, in which the order of perturbation will be automatically determined by a certain sort of convergence criteria.

In the space domain, one of the FEM, BEM and coupled BEM–FEM, with respect to practical cases, can be chosen combining with the perturbation scheme to describe the spatial variation of variables. FEM, for instance, is more suitable for the case, in which structures are inhomogeneous and include reinforcements in it.

In the recursive computation, the system matrix needs to be generated just one time in each of the time steps due to the time dependent material properties and only 'one step' coefficient vectors of variables at node points are required to be kept in storage.

The principle objective of this paper is to present a new approach for the solution of linear creep problems, in which a conventional assumption that variables remain constant or vary linearly within a discretised time interval is not adopted and the variation of variables in the time domain can, therefore, be described more precisely by exploiting the perturbation technique.

With the consideration of reinforcement, three kinds of perturbation based recursive formulae are derived, providing considerable flexibility to solve practical creep problems. Various numerical examples have been computed to verify the correctness of the methods presented. Comparison of numerical results with analytical solutions yields good correlation.

The overall approach presented has proved to be amenable to simultaneous discrete computing in the space and time domains and is capable of (i) describing the variation of variables which are not assumed to remain constant and vary linearly in a discretised time interval, (ii) dealing with reinforcement, time-dependent boundary conditions, etc., (iii) simulating coupled creep bodies with different ages. It is, therefore, proposed as a useful tool for solving the creep problems.

References

Arutyunyan, H.Kh., 1961. Some Problems in Creep Theory. Science Press, Beijing (in Chinese).

Brebbia, C.A., 1980. The Boundary Element Method for Engineers, 2nd ed. Pentech Press, London.

Christensen, R.M., 1982. Theory of Viscoelasticity, 2nd ed. Academic Press, New York.

Ouyang, H., 1989. Fundamental theory of long term deformation in concrete and its application. Doctoral thesis, Dalian University of Technology, Dalian, P.R. China.

Pan, D., 1980. Analysis of tunnel on linear visco-elastic theories. Chinese Journal of Tong-Hi University 3, 24–39.

Ponter, A.R.S., et al., 1981. Creep in Structures. Springer-Verlag, New York.

Wang, Y., 1984. Methodology of designing tunnel linings with the consideration of rheology. Chinese Journal of Underground Engineering 4, 26–34.

Wu, R., 1955. Unstable creep of a composite cylindrical tunnel with elastic medium. Transactions of the Academy of Science of Armenian Serial of Physical–Mathematical Science, T XII 3, 1103–1122 (in Russian).

Xie, Z., et al., 1983. The perturbation finite element method for solving problems with nonlinear material. Chinese Journal of Applied Mathematics and Mechanics 4 (1), 123–134.

Xie, Z., et al., 1984. The perturbation finite element method for solving nonlinear geometric problems. Chinese Journal of Applied Mathematics and Mechanics 5 (5), 709–722.

Yang, H., 1996. Application of finite volume method in 2-D problems of solid mechanics. Chinese Journal of Computational Structural Mechanics 14 (3), 333–341.

Yokoo, Y., Nakamura, T., Teuani, K., 1976. The increment perturbation method for large displacement analysis of elastic–plastic structures. Int. J. Numerical Method in Engineering 10 (3), 503–525.

Zeinkiewicz, O.C., 1971. The Finite Element Method in Engineering Science. McGraw-Hill, London.

Zeinkiewicz, O.C., 1975. An implicit scheme for a finite element solution of problems of viscoplasticity and creep. C/R/252/75, University College of Swansea, U.K.

Zhu, B., 1983. An implicity algorithm for the analysis of creep stress in concrete structures. Chinese Journal of Hydraulic Engineering 5, 40–46.